Biochemical and Biophysical Research Communications **278,** 34–37 (2000)
doi:10.1006/bbrc.2000.3756, available online at http://www.idealibrary.com on IDEAL®

Blockage of Human T Lymphocyte Kv1.3 Channels by Pi1, a Novel Class of Scorpion Toxin

Mózes Péter, Jr.,* Péter Hajdu,* Zoltán Varga,* Sándor Damjanovich,* Lourival D. Possani,† György Panyi,* and Rezsö Gáspár, Jr.*,[1]

**Department of Biophysics and Cell Biology, Medical and Health Science Center, University of Debrecen, Debrecen, 4012 Hungary; and †Department of Molecular Recognition and Structural Biology, Institute of Biotechnology, National Autonomous University of Mexico, Cuernavaca 62210, Mexico*

Received October 6, 2000

Using the patch-clamp technique we determined that *Pandinus imperator* toxin Pi1, a recently described peptide toxin having four disulfide bridges instead of the usual three in scorpion toxins, blocked Kv1.3 channels of human T lymphocytes from the extracellular side with a 1:1 stoichiometry. Kv1.3 block was instantaneous and removable with toxin-free extracellular solution. The toxin did not influence activation or inactivation of the channels. We found that Pi1 blocked Kv1.3 with less affinity (K_d = 11.4 nM) than the structurally related three disulfide bridge containing toxins Pi2 (50 pM) and Pi3 (0.5 nM). The fourth disulfide bridge in Pi1 had no influence on the channel binding ability of the toxin; the less effective block was due to differences in amino acid side chain properties at positions 11 and 35.

Scorpion toxins are useful pharmacological probes for studying the biological function of voltage-gated K^+ channels. In search for new K^+ channel inhibitors the effect of the whole venom of the scorpion *Pandinus imperator* and some of its peptide toxin components have been tested on K^+ channels of different origin and found to block a variety of them, including Kv1.3 of human peripheral blood lymphocytes, with different affinities (1–5).

K^+ channel blocking scorpion toxins (Stox) are short peptides about 31 to 39 amino acids. Their primary structure is highly variable, except for the constant relative position of cysteines and some other residues. The three-dimensional structure of the K^+ channel blocking Stox have some common motifs, their structures are usually stabilized by three disulfide bridges. Recently, a new structural class of K^+ channel blocking Stox has been discovered presenting a fourth disulfide bond (6, 7). Pi1, a member of the *Pandinus imperator* toxins, belongs to this class (1, 4). The pairing of the usual three disulfide bridges is conserved in two members of the new Stox family, namely in Pi1 and HsTX1, but not in maurotoxin, the third member of the family. The overall folding of Pi1 and maurotoxin are similar to that of the three disulfide bridge containing Stox, however in Pi1 the fourth disulfide bridge connects the loop between the alpha-helix and the beta-sheet structures to the C-terminus (6, 7). In two other peptide toxins, Pi2 and Pi3, form the *Pandinus* venom and also in noxiustoxin the amino-terminal regions were found important for the recognition of potassium channels (2).

In the present study we examine the effect of *Pandinus* toxin Pi1 on the whole-cell K^+ currents of human peripheral blood T lymphocytes by the patch-clamp method. The results are compared to those of *Pandinus* toxins Pi2 and Pi3 and discussed in the view of the structural differences between the toxins. The predominant voltage-gated potassium channel underlying whole-cell K^+ currents of human lymphocytes is the *Shaker* Kv1.3.

MATERIALS AND METHODS

Cell isolation. Heparinized human peripheral venous blood was obtained from healthy volunteers (authors of the paper). Mononuclear cells were separated by Ficoll–Hypaque density gradient centrifugation. Collected cells were washed twice with Ca^{2+}- and Mg^{2+}-free Hanks' solution containing 25 mM Hepes (pH 7.4). Cells were cultured in a 5% CO_2 incubator at 37°C in 24-well culture plates in RPMI 1640 supplemented with 10% FCS (Hyclone, Logan, UT), 100 U/liter penicillin, 100 μg/ml streptomycin and 2 mM L-glutamine at 0.5×10^6/ml density for 3–4 days. The culture medium also contained 2.5 or 5 μg/ml of phytohemagglutinin A (PHA-P, Sigma–Aldrich Kft, Hungary) to increase K^+ channel expression (8, 9).

Electrophysiology. Whole-cell measurements were carried out using Axopatch-200 and Axopatch-200A amplifiers connected to personal computers using Axon Instruments TL-1-125 and Digidata 1200 computer interfaces, respectively. For data acquisition and analysis the pClamp6 software package (Axon Instruments Inc.,

[1] To whom correspondence should be addressed. Fax: +36-52-412623. E-mail: gaspar@jaguar.dote.hu.

0006-291X/00 $35.00

Foster City, CA) was used. T lymphocytes were selected for current recording by incubation with mouse anti-human CD2 (Becton–Dickinson, San Jose, CA) followed by selective adhesion to petri dishes coated with goat anti-mouse IgG antibody (Biosource, Camarillo, CA), as described by Matteson and Deutsch (9). Dishes were washed gently five times with 1 ml of normal extracellular bath medium (see below) for the patch-clamp experiments. Standard whole-cell patch-clamp techniques were used (5, 10–12). Series resistance compensation up to 85% was used to minimize voltage errors and achieve good voltage clamp conditions ($V_{err} < 5$ mV). Pipettes were pulled from GC 150 F-15 borosilicate glass capillaries (Clark Biomedical Instruments, UK) in two stages and fire polished resulting in electrodes having 2–3 MΩ resistance in the bath. The bath solution was (in mM): 145 NaCl, 5 KCl, 1 $MgCl_2$, 2.5 $CaCl_2$, 5.5 glucose, 10 Hepes. The measured osmolarity of the external solutions was between 302 and 308 mOsm. The pipette solution was (in mM): 140 KF, 11 K_2EGTA, 1 $CaCl_2$, 2 $MgCl_2$, and 10 Hepes (pH 7.20, ~295 mOsm).

Test substances. *Pandinus imperator* venom (PiV) was obtained from anesthetized animals by electrical stimulation. To separate the peptide toxin component Pi1 the soluble venom was initially fractionated in a Sephadex G-50 column and subfractions were further separated by high performance liquid chromatography (HPLC), using a C18 reverse-phase column (Vydac, Hesperia, CA), of a Waters 600E HPLC apparatus. The homogeneity of the purified samples was confirmed by step-gradient HPLC and direct Edman degradation using an automatic sequencer (2). Solutions were supplemented with 0.1 mg/ml bovine serum albumin to suppress nonspecific binding of the toxin to the walls of the tubes and to the petri dish. Bath perfusion around the measured cell with different test solutions was achieved using a gravity-flow perfusion setup with 8 input lines and PE10 polyethylene tube output tip having flanged aperture to reduce the turbulence of the flow. Excess fluid was removed continuously. For the measurement of blocking properties of the toxin, data acquisition was synchronized to fluid exchange using solenoid valves controlled by pClamp6 via digital outputs of Digidata 1200. The reference electrode was connected to the recording chamber with an agar bridge to eliminate junction potential changes during perfusion.

RESULTS AND DISCUSSION

Figure 1A illustrates that human peripheral blood T lymphocytes display strong outward whole-cell currents on step depolarization from a −100 mV holding potential. After reaching a peak, the current declines due to inactivation toward a low steady state value. Ion channels basically contributing to this transient outward current have been identified as voltage-gated potassium channels of type Kv1.3 on the basis of being selective for K^+, having a linear single-channel current–voltage relationship with an approximate slope conductance of 10–12 pS at pipette potentials between −30 to +40 mV.

Peak values of the T lymphocyte whole-cell currents were significantly reduced by 10 nM Pi1 in the external bath, although no significant alteration in the activation and the inactivation rate of the K^+ current was observed in the presence of the toxin (see Figs. 1A and B). Pi1 merely scaled down the currents without altering its kinetics. This suggests that Pi1 has no effect on the gating of the underlying Kv1.3 channels, the reduction of current is most probably due to the blockade of the flow of potassium through Kv1.3. A simple blocking

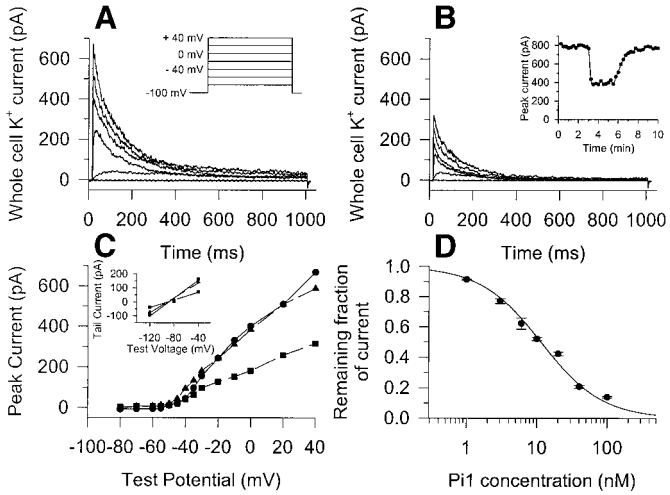

FIG. 1. Externally applied Pi1 reversibly blocks whole-cell K^+ currents in human T lymphocytes. (A) Control current traces elicited by voltage steps (inset) lasting for 1000 ms and applied every 80 s from a holding potential of −100 mV to various potentials from −80 to +40 mV. Only selected traces are displayed for picture clarity. (B) The same cell during bath perfusion with 10 nM Pi1; (inset) time course of the development and removal of K^+ channel block by the application of external 10 nM Pi1 and successive washing of the cell with toxin-free ECS via a direct perfusion system to the cell. The current values displayed were evoked by 6 ms long +50 mV depolarizing pulses from a −100 mV holding potential. (C) Effect of extracellular Pi1 on peak current–voltage relations of whole-cell K^+ currents (●, control; ■, 10 nM Pi1; ▲, wash-out). No leak subtraction has been applied. (Inset) 10 nM Pi1 has no effect on the reversal potential of the whole-cell K^+ current of human lymphocytes. In this experiment the currents were activated by 6-ms (duration) voltage steps to +40 mV at regular intervals of 40 s from a holding potential of −100 mV, then current traces were initiated by step-backs to the given more negative potentials. Current values belonging to starting points of these current traces are displayed at selected potentials. (D) Dose dependence of K^+ channel block by Pi1 in human lymphocytes ($n = 4$, mean ± SEM). The remaining fraction of whole-cell current (R_f) values are based on peak current values measured at +40 mV test potential before (I_{K0}) and after (I_K) the administration of the given dose of Pi1 ($R_f = I_K/I_{K0}$). Fitted curve is based on a 1:1 stoichiometry channel:toxin interaction model.

mechanism of Kv1.3 by Pi1 is further supported by the insert of Fig. 1C, which shows that Pi1 has no effect on the reversal potential of the whole-cell current (13).

Pi1 block of the T lymphocyte Kv1.3 channels is voltage independent at test potentials more positive than −20 mV. This is best seen in Fig. 1C, where the peak current vs voltage relationship (I–V) is shown for currents in Figs. 1A and B, as well as after wash-out of the toxin. The absence of appreciable voltage dependence in the Pi1 block indicates that this peptide binds to the most external region of the Kv1.3 channel, where the highly charged toxin molecule does not sense the transmembrane electrical field. By analogy with the known blocking mechanism of other K^+ channel toxins, Pi1 binding should most probably happen in the outer mouth of the channel pore (4).

TABLE 1

Primary Structures of Pi1, Pi2, Pi3, and ChTx*

																						**																**
				1	2	3	4	5	6	7	8	9	10	11	12	13	14	15	16	17	18	19	20	21	22	23	24	25	26	27	28	29	30	31	32	33	34	35
Pi1				L	V	K	C	R	G	T	S	D	C	G	R	P	C	Q	Q	Q	T	G	C	P	N	S	K	C	I	N	R	M	C	K	C	Y	G	C
Pi2				T	I	S	C	T	N	P	K	Q	C	Y	P	H	C	K	K	E	T	G	Y	P	N	A	K	C	M	N	R	K	C	K	C	F	G	R
Pi3				T	I	S	C	T	N	E	K	Q	C	Y	P	H	C	K	K	E	T	G	Y	P	N	A	K	C	M	N	R	K	C	K	C	F	G	R
	1	2	3	4	5	6	7	8	9	10	11	12	13	14	15	16	17	18	19	20	21	22	23	24	25	26	27	28	29	30	31	32	33	34	35	36	37	
ChTx *p*	E	F	T	N	V	S	C	T	T	S	K	E	C	W	S	V	C	Q	R	L	H	N	T	S	R	G	K	C	M	N	K	K	C	R	C	Y	S	

* Structures were aligned in search for best similarity in the amino acid sequences of these peptides.
** Cysteines corresponding to the fourth disulfide bridge in Pi1.

The full development of the blocking effect of Pi1 was rather quick (see Fig. 1B, inset). After the application of 10 nM extracellular Pi1 to the cells, the peak whole-cell K^+ current value evoked by short (6 ms) depolarizing pulses to +40 mV stabilized at a reduced level within approximately the time of the 15-s interpulse interval applied, a value corresponding to the time needed for the complete recovery of the channels after the 6 ms long +40 mV pulses. Perfusion of the bath with toxin-free extracellular solution for approx 2 min resulted in a recovery of the whole-cell currents (see Fig. 1B, inset).

Several successful blocking experiments were performed with various other Pi1 concentrations in the 1–100 nM range. In this concentration range the block was dose dependent and the experimental data could be fitted to a channel-toxin interaction model, where one channel protein binds one toxin molecule. Based on this assumption the remaining fraction (R_f) of the whole-cell current at a given toxin concentration was expressed by the following equation: $R_f = K_d/(K_d + [\text{Pi1}])$, which was fitted to the measured data points yielding 11.4 nM for the half blocking concentration of Pi1. In the above equation $R_f = I_K/I_{K0}$, where I_{K0} and I_K are the initial and Pi1 blocked current amplitudes, respectively, K_d is the dissociation constant and [Pi1] is the toxin concentration.

Comparison of the 11.4 nM half blocking concentration of Pi1 to preliminary K_d values of 50 pM and 0.5 nM, published for the three disulfide bridge containing *Pandinus* toxins Pi2 and Pi3, respectively shows that the four disulfide bridge containing Pi1 is the least effective toxin in the group (5). All three toxins are structurally closely related to ChTX as can be seen in Table 1. The ^{1}H NMR structural investigation of Pi1 showed that despite some divergence in the primary sequence and the presence of an additional disulfide bridge, Pi1 exhibits the same basic structural motifs found in ChTX and some other important K^+ channel blocking toxins including MgTX (14). Molecular modeling of Pi1, Pi2 and Pi3 showed that the backbone fold of these toxins is virtually identical to that of ChTX (3). Backbone folding and consequently the presence of the fourth disulfide bridge do not affect the accessibility of Lys24 (Lys27 in ChTX), a residue shown to be essential for tight binding of ChTX to the channel receptor, to Kv1.3 in Pi1. The observed differences in the Kv1.3 blocking ability of Pi1 and the other Pi's are most likely due differences in side chains and surface charge (see Table 1). The change of Tyr to Gly at position 11 and replacement of Arg with Cys at position 35 may play key roles because docking of the Pi toxins to a K^+ channel model showed that these amino acids are exposed at critical positions compared to the binding surface of the channel (3). The Arg to Cys change at position 35 also induces a large change in the local surface charge, because the positively charged Arg side chain is replaced by the negatively charged carboxyl-terminal in Pi1.

In summary, the fourth disulfide bridge in Pi1 did not influence the binding ability of the toxin to the Kv1.3 channels in human T lymphocytes. The less effective Kv1.3 block by Pi1 compared to Pi2 and Pi3 is due to differences in amino acid side chain properties at positions 11 and 35. Pi1 might be still an advantageous Kv1.3 blocker against its hindered channel binding ability, because the fourth disulfide bridge may confer extra stability to this peptide.

ACKNOWLEDGMENTS

This work was supported by Grants ETT T05/102/2000, OTKA T029947, and FKFP 327/2000 to R.G., OTKA T30411 to S.D., FKFP 622/2000, OTKA F035251, and US–Hungarian Joint Found No. 542 to G.P., and Grant 75197-527107 from the Howard Hughes Medical Institute to L.D.P.

REFERENCES

1. Olamendi Portugal, T., Gomez Lagunas, F., Gurrola, G. B., and Possani, L. D.. (1996) *Biochem. J.* **315,** 977–981.
2. Gomez Lagunas, F., Olamendi Portugal, T., Zamudio, F. Z., and Possani, L. D. (1996) *J. Membr. Biol.* **152,** 49–56.
3. Rogowski, R. S., Collins, J. H., O'Neill, T. J., Gustafson, T. A., Werkman, T. R., Rogawski, M. A., Tenenholz, T. C., Weber, D. J., and Blaustein, M. P. (1996) *Mol. Pharmacol.* **50,** 1167–1177.
4. Gomez Lagunas, F., Olamendi Portugal, T., and Possani, L. D. (1997) *FEBS Lett.* **400,** 197–200.
5. Péter, M., Varga, Z., Panyi, G., Bene, L., Damjanovich, S., Pieri,

C., Possani, L. D., and Gáspár, R., Jr. (1998) *Biochem. Biophys. Res. Commun.* **242,** 621–625.

6. Possani, L. D., Selisko, B., and Gurrola Briones, G. (1999) *Perspect. Drug Discovery Design* **15/16,** 15–40.
7. Savarin, P., Romi-Lebrun, R., Zinn-Justin, S., Lebrun, B., Nakajima, T., Gilquin, B., and Menez, A. (1999) *Protein Sci.* **8,** 2672–2685.
8. Deutsch, C., Krause, D., and Lee, S. C. (1986) *J. Physiol. (London)* **372,** 405–423.
9. Matteson, D. R., and Deutsch, C. (1984) *Nature* **307,** 468–471.
10. Gáspár, R., Jr., Panyi, G., Krasznai, Z., Ypey, D. L. Vereb, G., Pieri, C., and Damjanovich, S. (1994) *Mol. Pharmacol.* **46,** 762–766.
11. Varga, Z., Bene, L., Pieri, C., Damjanovich, S., and Gáspár, R., Jr. (1996) *Biochem. Biophys. Res. Commun.* **218,** 828–832.
12. Gáspár, R., Jr., Varga, Z., Bene, L., Maracheselli, F., Pieri, C., and Damjanovich, S. (1996) *Biochem. Biophys. Res. Commun.* **226,** 303–308.
13. Hille, B. (1992) Ionic Channels of Excitable Membranes, 2nd ed., p. 347. Sinauer, Sunderland, MA.
14. Delepierre, M., Prochnicka Chalufour, A., and Possani, L. D. (1997) *Biochemistry* **36,** 2649–2658.